Facile fabrication of amino-functionalized porous materials for Pb^{2+} removal

Y. ZHAO, S. ZHAI[*], B. ZHAI, Q. AN[*]
Faculty of Light Industry and Chemical Engineering, Dalian Polytechnic University, Dalian 116034

A facile sol-gel strategy was employed to fabricate amino-functionalized hybrid xerogels using mono-, di-, tri-amino-organoalkoxysilanes, polymeric polymethlhydrosiloxane (PMHS) and tetraethylorthosilicate (TEOS) as co-precursors without traditional structure-directing agents. The loadings of amino moieties of the amino-functionalized xerogels could be tuned from 5% to 30% by adjusting the molar ratio of organoalkoxysilane/ silica in the synthesis system. The N$_2$ sorption isotherms, SEM, and TEM techniques revealed that these as-prepared hybrids possess typical wormhole-like framework structures with high specific surface area (~ 532 m^2/g), large pore volumes (~ 0.99 cm^3/g) and relatively narrow pore diameter (~ 7.5 nm). The NMR, FT-IR, TG-DTG and elemental analysis indicated that amino groups had been successfully introduced into the final xerogel-like samples, and the content could be variable from 0.36 to 5.03 mmol/g. The adsorption of Pb^{2+} experiments were conducted batchwise in water at room temperature. The results showed that adsorption capacity increased with the concentration of amino groups in the functionalized xerogel, and the maximum adsorption capacities of 176, 176 and 193 mg/g were obtained using mono-, di- and tri-amino-functionalized adsorbents, respectively. These results implied that the accessibility of the amino groups introduced to the framework via the sol-gel condensation method were different.

1. Introduction

Organic-inorganic hybrid materials with developed frameworks have been a center of interest for years due to their narrow pore size distribution and high specific surface area [1,2] and high density of active sites dispersed throughout the framework. These materials offer many advantages over other solids due to their interesting textural properties, hydrothermal stability and pore size tailoring. Therefore, hybrid porous silicas have recently found many applications in separation and pre-concentration of metal ions for analytical purposes[3], environmental de-pollution of toxic heavy metals [4] and adsorption of organic substances[5] from aqueous solutions. However, these applications require modification of the internal surface of the mesoporous silicas using several strategies to assign specific properties and reactivity. Among these strategies, surface functionalization via tethering of organic functional groups is of much interest due to the introduction a number of functionalities onto the internal pore surfaces [1]. Therefore, organic functional groups such as amine, thiol, carboxylic, alkyl chloride, and aromatic have been incorporated into the structure of siliceous materials via post-synthesis grafting or co-condensation. Among all these organic functional groups, several investigations were dedicated to surface modification of different mesoporous silicas using aminoalkoxysilanes for their application in catalysis[6] as well as environmental pollution control[7]. In this regard, different amino-functional groups including mono-, di- and tri-amines proved to be potential adsorbents for heavy metal cations such as mercury, lead, cobalt, copper and zinc cations from water [8], organic molecules [9] as well as CO$_2$ from gaseous emissions [10]. Furthermore, protonated amino-functionalized mesoporous silicas were applied for the adsorptive removal of different pollutant anions from water such as chromate, arsenate and selenate [11], as well as nutrient anions, namely nitrate and phosphate [12]. Functionalized porous frameworks with a high density of amino groups and defined mesochannels that can enhance the accessibilities of molecules have been applied to solid-base catalysts for Knoevenagel and aldol condensations [13], and fascinating adsorbents for heavy metal cations, such as cobalt, copper and zinc, causing environmental problems [14]. However, a vast majority of amino-functionalized hybrid porous silicas were prepared employing surfactants as pore-forming agents, which made the whole process somewhat time-consuming, cost-ineffective as the high cost of surfactant, and potential environmental impact of acidified alcoholic media for surfactant extraction. The fabrication of amino-functionalized adsorbents that present high surface areas and controlled pore size distributions using one-step sol-gel method will be helpful to expand the application in environmental field especially for selective adsorption [15].

In this paper, we report on a facile preparation method that amino-functionalized hybrid adsorbents could be assembled using a polymeric PMHS-assisted sol-gel

process in the absence of traditional surfactants; and the textural properties of amino-functionalized hybrids made from mono-, di-, tri-amino-organoalkoxysilanes were investigated using various techniques. Besides this, our present investigation is intended to study the adsorption of Pb^{2+} using amino-functionalized adsorbents and to investigate comparatively the difference of the one, two and three amino groups on the pore structures and the adsorption capacity of Pb^{2+} from aqueous solutions.

2. Experimental

2.1 Chemicals

3-Aminopropyltrimethoxysilane [$H_2N(CH_2)_3Si(OCH_3)_3$, **N**-silane, purity >99%], N-[3-(trimethoxysilyl)propyl]ethylenediamine [$(CH_3O)_3Si(CH_2)_3NHCH_2CH_2NH_2$, **NN**-silane, purity > 98%] and 3-[2-(2-Aminoethylamino)ethylamino]propyl [$(CH_3O)_3Si(CH_2)_3NHCH_2CH_2NHCH_2CH_2NH_2$, **NNN**-silane, purity > 98%] were purchased from Aldrich. Polymethlhydrosiloxane (PMHS) (purity > 99%, M_w = 2700-5400), was provided by Gelest company. Tetraethylorthosilicate (TEOS, purity > 99%), ethyl alcohol and sodium hydroxide (NaOH) were provided by Tianjin chemical corporation of China. Lead (II) nitrate Pb(NO$_3$)$_2$ (purity > 99.0%) was supplied by Tianjin fine chemical industry research institute. All the chemicals were used as received without further purification.

2.2 Synthesis

The synthesis of amino-functionalized hybrid materials using sol-gel co-condensation method was conducted as follows. In a typical synthesis, 0.76 mL of PMHS was dripped into a flask containing certain amount of ethanol (70 mL) and NaOH (0.08 g). The initial gel composition was (1-x) TEOS: x N silane, where x is the proportion of the N silane as mono-amino group in the Si sources. After continuous stirring for 24 h, 4 mL deionized water was added into the system and kept vigorous stirring for another 3 h. After being aged for 2~5 d under ambient conditions, the sol converted into wet gel. The solvent were removal by treatment at 80 ^{o}C for 24 h and glass-like solids were finally obtained, which can be used to adsorb Pb^{2+} after careful washing with deionized water. NN and NNN silanes were also used as sources of di- and tri-amino groups for the synthesis of the functionalized hybrid xerogels. The amino-functionalized xerogels prepared with different amount of N, NN and NNN silanes were correspondingly designated as x-N-, x-NN- or x-NNN-M, respectively, where x was the proportion of the amino-organoalkoxysilane in the Si source.

2.3 Characterization

Nitrogen adsorption-desorption experiments were performed at 77 K using a Quantachrome Autosorb NOVA 2200e volumetric analyzer. Prior to analysis, the materials were degassed at 180 ^{o}C for 4 h in vacuum. The specific surface area, S_{BET}, was determined from the linear part of the BET plot (P/P$_0$ = 0.05-0.20). The pore size distributions were calculated from the desorption branch using the Barrett-Joyner-Hallenda (BJH) [14]. The total pore volume was evaluated from the adsorbed amount at a relative pressure of about 0.99.

The morphology of the amino-functionalized xerogels was determined with a SEM (JEOL 6400). Transmission electron microscopy (TEM) image was obtained by a JEOL 2010 electron microscope with an acceleration voltage of 200 kV.

The content of total amino groups in the amino-functionalized hybrid composites was determined by the CHN elemental analysis, which was performed using a Perkin-Elmer 240C elemental analyzer (Perkin-Elmer Corp.).

Thermogravimetric analyses were conducted in a Netzsch STA 409 PC equipment. Approximately 10 mg of sample were weighed in an alumina crucible and heated at 30-700 ^{o}C, at the heating rate of 10 ^{o}C min^{-1} under nitrogen flow (30 cm^3 min^{-1}).

Fourier transform infrared (FT-IR) transmission spectroscopy was taken on a Bruker IFS 66V/S spectrometer in the region 4000 to 400 cm^{-1}, in KBr discs.

The solid-state NMR experiments were carried out at B$_0$ = 9.4 T on a Bruker AVANCE III 400 WB spectrometer at Testing Center of Yangzhou University. The corresponding resonance frequencies of ^{29}Si was 79.5 MHz. Samples were packed in a 7 mm ZrO$_2$ rotor and spun at the magic angle (54.7^o), and the spin rate was 4 kHz. ^{29}Si MAS NMR spectra were acquired using a 45° pulse of 2.5 μs and a recycle delay of 20 s. The ^{29}Si chemical shifts were referenced to the high field resonance of kaolinite at -91.5 ppm.

2.4 Adsorption of Pb^{2+} tests

In order to test the metal removal ability of the prepared materials, the adsorption tests were performed batchwise in 100 mL stirred flasks at room temperature. Typically, 0.1 g of amino-functionalized adsorbent was added in a flask of 50 mL of aqueous solution of Pb^{2+}. The initial concentration for these experiments was 400 mg/L and the metal salt used was nitrate of Pb(NO$_3$)$_2$. After 12 h of vigorous stirring assuring equilibrium and then filtered to collect the final solutions. The remaining metal content was determined by a Hitachi 180-80 spectrometer after calibration with stock solution in the range of concentration of 0-10 mgL^{-1}. The emission lines used were according to the standard EPA method for analysis of these metals [26]. Adsorbed heavy metal amount was determined by difference between initial and final metal concentrations in the solution.

3. Results and discussions

3.1 Analysis of N-, NN- and NNN-M

Amino-functionalized xerogels with developed porosities could be facilely prepared by one-pot co-condensation of N-, NN-, NNN-silane, TEOS and PMHS in the absence of traditional templates, by which tedious preparation procedures were favorably avoided. The textural properties of the materials were investigated through N_2 adsorption–desorption isotherms and pore size distribution curves, as displayed in Fig. 1 and Table 1. According to the IUPAC classification, non-functionalized sample 0-N-M displays a typical Type IV isotherm with a pronounced of hysteresis loops between 0.6-0.9, which is attributable to capillary condensation process of nitrogen molecules [16]; it indicates that there existence of cylindrical pore channels in the sample as previously reported results [17]. In contrast, except for 30%-NN-M, amino-functionalized samples with amino groups content up to 20% exhibit hysteresis loops with an intermediate shape between H1 and H2 types, demonstrating the existence of cylindrical pore channels and the reduction of both the porosity and pore size of the functionalized samples with increasing amino groups content. Meanwhile, framework-confined mesoporosity and a small partition of textural mesoporosity were also observed in these materials [17].

Accordingly, the BJH pore size distributions calculated from desorption branches of the isotherms are shown in Fig.1b, and the structural parameters are listed in Table 1. It is clear that all samples possess a narrow pore size distribution with a peak centered at 7.5 7.3, 7.0, 6.8, 6.2 nm, respectively, with the increase in the proportion of NN silane from 0 to 30 mol%. Both specific surface area and pore volume slightly decrease upon modification with the increase of amino content, due to the space occupied by the aminopropyl chains bound on the inner surface of mesopores [18]. The surface area and pore volume change from 696 to 265 m^2g^{-1} and 1.27 to 0.5 cm^3g^{-1}, respectively.

Utilizing the similar method, we also synthesized the N- and NNN-functionalized xerogels, through which a similar trend of changes of textural properties were also clearly observed as NN-M. Owing to the fact that the molecular sizes of N-, NN- and NNN-silane are estimated to be approximately 0.9, 1.3 and 1.7 nm [19], respectively, the pore size narrowing induced upon the hybrid materials proved to be dependent on the type of amino-organoalkoxysilane used, as evidenced in Table 1. Furthermore, along with the increase from 5 to 30%, the surface area decreased monotonically from 494 to 146 m^2g^{-1} (N-M) and 560 to 10 m^2g^{-1}(NNN-M), and the pore size from 6.6 to 3.5 nm (N-M) and 7.5 to 3.0 nm (NNN-M). The decrease is mainly dependent on the size of incorporated amino ligands, i.e., the highest decrease being obtained for the materials functionalized using the most bulky organoalkoxysilane (NNN-silane). Also the decrease was dependant on the coverage as well since the highest decrease in BET surface area was recorded for the highest ratios organoalkoxysilane to silica used in the

co-condensation procedure. These results suggest that NNN silanes are a little more difficult to condense into the siloxane network due to the larger size of the hydrophilic terminal organic moiety in these silanes than that in N silane. This behavior can be directly correlated to the pore size narrowing discussed above and was observed for several mesoporous materials modified using different organic ligands [2,3]. It has been observed that the high content of organoalkoxysilanes in the Si sources hampered the condensation of silicates to form the framework because the rate of hydrolysis of organoalkoxysilanes is slower under basic conditions than that of tetraalkoxysilanes due to the higher basicity at the silicon center [20].
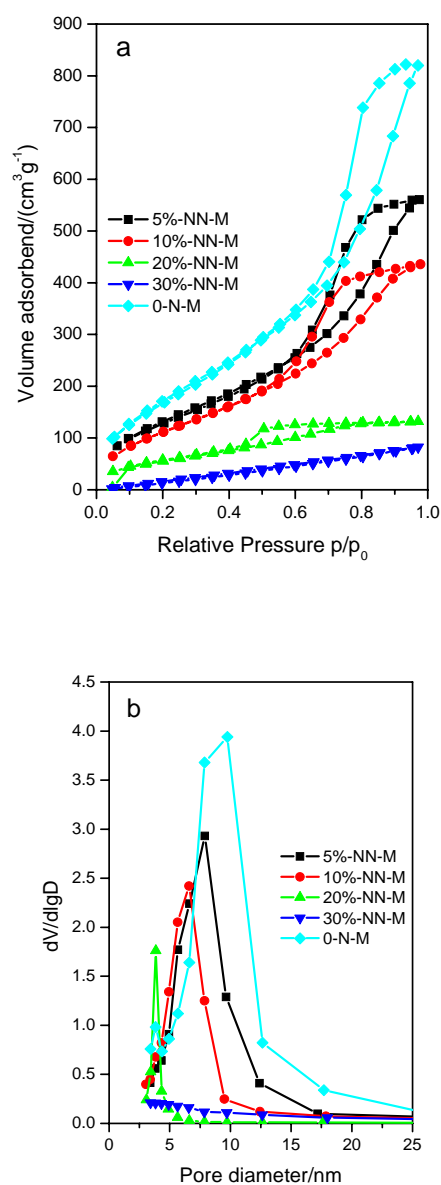

Fig.1. N_2 adsorption-desorption isotherms and pore size distribution curves of hybrid xerogels

The N molar content of the synthesized samples was

analyzed and the results are included in Table 1. Clearly, the incorporation amount is mainly associated to the ratio of amino-bearing silanes to TEOS, and the amino group loadings in final xerogels significantly increase with usage of precursors in the synthesis. Furthermore, for the same molar ratio orangoalkoxysilane/silica of 20%, the elemental analysis indicated a nearly similarly effective incorporation for N, NN and NNN-M xerogels, respectively. Similar trend was previously reported by Bios et al. [21] for mesoporous HMS materials. Moreover, irrespective of the organic functional group, the incorporation efficiency is slightly decreased with increasing the ratio of orangoalkoxysilane/silica in the synthesis system.

The functional groups contained in the xerogels were investigated using FT-IR technique. The IR patterns of the hybrid materials before and after modification are shown in Fig. 2 for the materials prepared with monoamine-, diamine- and triamine-bearing precursors. It is noticeable that, for all samples, the bonds at 781 cm^{-1} and 1075 cm^{-1} can be assigned to the symmetric and asymmetric stretching vibration of Si-O-Si, respectively; these reflections are typical groups found on the surface of silica materials [22]. Besides, the peak at 1630 cm^{-1} is due to the stretching vibration of Si-OH, and the bonds at ca. 2990 cm^{-1} are associated to the -C-H stretching vibration of -CH$_3$ and -CH$_2$- groups derived from PMHS and amino-alkyloxysilanes.

By contrast, distinct difference can be observed over amino-functionalized materials. Firstly, new bands around 1430-1470 cm^{-1} are present and become more intense from 20%-N-, NN-M to 20%-NNN-M, which can be attributed to the NH$_2$ stretching vibration, illustrating amino groups

have been introduced into the hybrid composites. Secondly, from 0-N, 20%-N-, NN- to NNN-M, the bands of aliphatic C-H stretching vibration exhibit improved intensity which once indicates the existence of amine ligands on pore surface of as-prepared hybrid materials and in agreement with the elemental analysis results listed in Table 1.

Table 1. Structural properties of amino-functionalized xerogels synthesized using co-condensation sol-gel method.

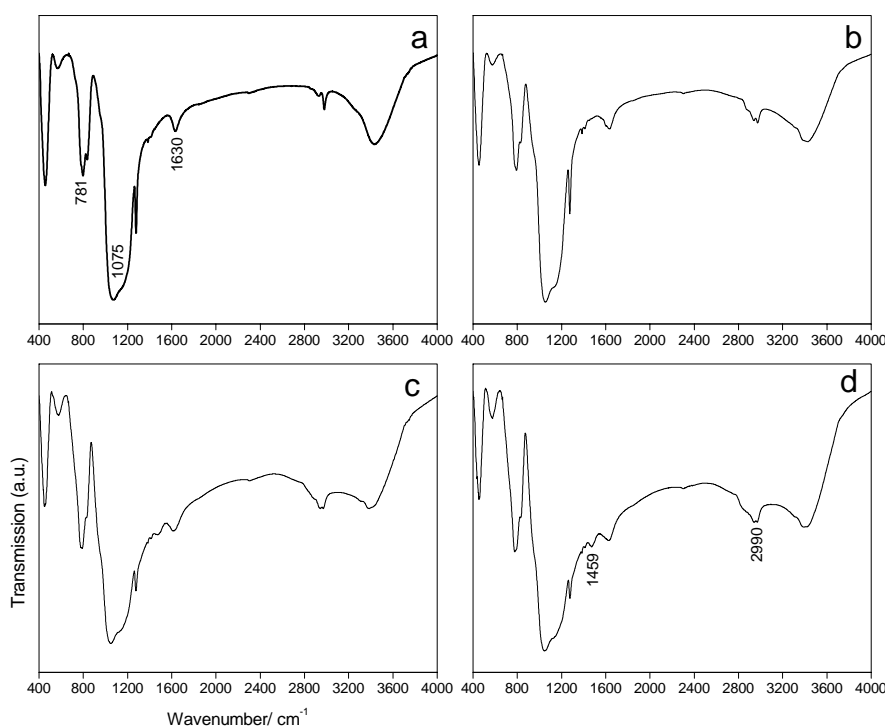| Samples	Amino group /mmol g^{-1}	BET surface area /m^2 g^{-1}	Total pore volume /cm^3 g^{-1}	Average pore diameter /nm
0-M(non-amino)	—	696	1.27	7.5
5%-N-M	0.36	532	0.99	7.3
10%-N-M	0.69	469	0.82	7.0
20%-N-M	1.64	320	0.68	6.8
30%-N-M	2.21	265	0.50	6.2
5%-NN-M	0.98	560	0.87	6.6
10%-NN-M	2.10	403	0.58	6.2
20%-NN-M	3.11	158	0.15	3.8
30%-NN-M	4.14	16.3	1.4×10^{-2}	3.5
5%-NN-M	1.08	494	1.04	7.5
10%-NN-M	2.30	376	0.61	6.0
20%-NN-M	3.72	274	0.21	3.1
30%-NN-M	5.03	10.0	7.7×10^{-3}	3.0

Fig.2. FT-IR spectra of hybrid xerogel materials of 0-N-M, 20%-N-M, 20%NN-M and 20%-NNN-M

Solid state ^{29}Si MAS NMR of representative 20%-NN-M is depicted in Fig. 3. It is clear that the spectrum displays essentially two clear resonance peaks at -110 ppm (Q^4) and -101 ppm (Q^3) assignable to fully condensed silica and silica with one terminal hydroxyl as well as a weak signal at -90 ppm assigned to Q^2 units. Besides, two signals at -58 ppm and -65 ppm attributed to T^2 [RSi(OSi)$_2$OH] and T^3 [RSi(OSi)$_3$] resonances [23], respectively, were observed over this sample; the presence of the T^m peaks indicates the introduction of organic functional moieties into the silica skeleton, which are originated from both polymeric PMHS and aminoalkyloxysilane sources, demonstrating the co-condensation of tri-constituent of silica precursors at the molecular level.
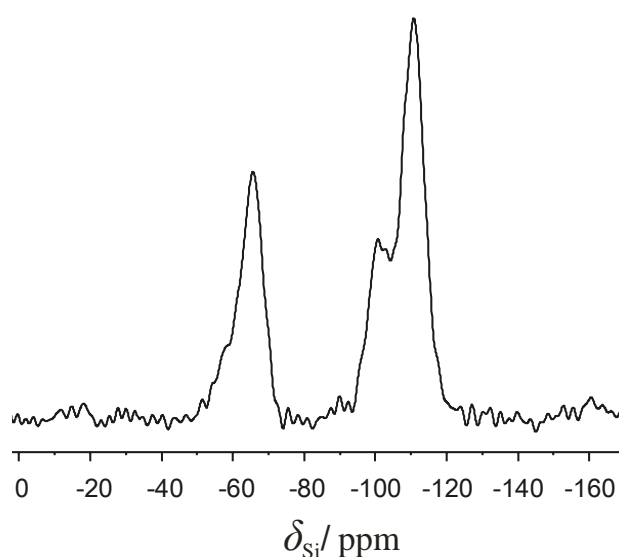

Fig.3. ^{29}Si MAS NMR of as-prepared 20%-NN-M xerogel sample.

To further elucidate the detailed structures of hybrid materials, Fig. 4(a) and (b) illustrate the TEM and SEM images of typical sample 20%-NN-M synthesized employing the non-surfactant sol-gel pathway. As can be seen from Fig. 4(a), the sample is composed of glass particles with irregular shapes, being analogous to the conventional silica xerogel prepared in the alcohol-rich system without traditional surfactants [24] and depicts a direct image of a typical 3D "wormhole-like" pore frameworks, which is similar to those pore configuration of MSU-n type porous silicas without long-range ordering [25]. Besides, the morphology of sample 20%-NN-M characterized by SEM is shown in Fig. 4(b). It is seen that the xerogel is composed of irregular and stone-like particles, and this observation is similar to the conventional silica xerogels obtained under ambient conditions [24]. The combination of N$_2$ adsorption-desorption and TEM analysis results confirmed that the amino-functionalized hybrid materials have a mesoporous structure. It should be noted that, even though the material is composed of disordered pore arrays viewed

through TEM image, the pore channels are easily accessible and relatively uniform as illustrated by the pore size distribution curve in Fig. 1b.
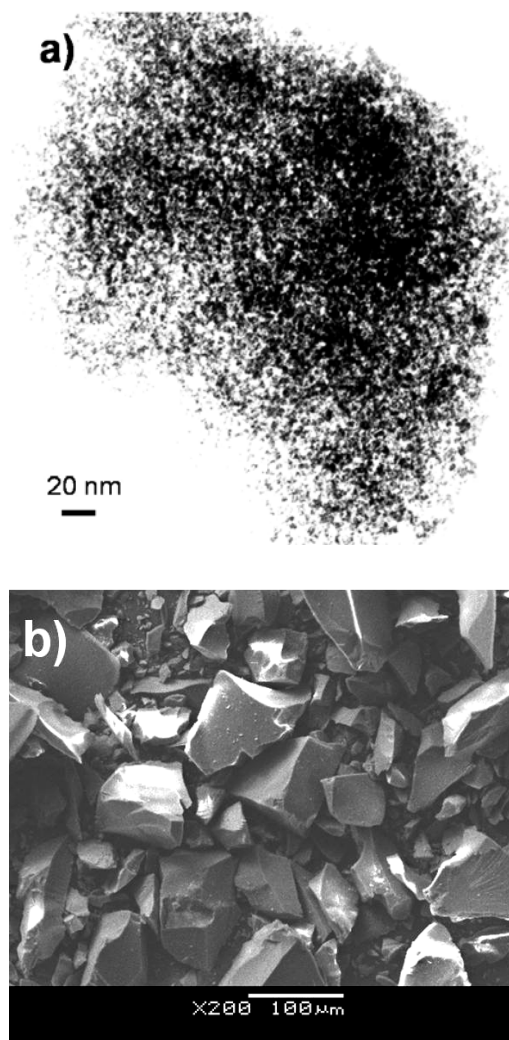

Fig.4. TEM (a) and SEM (b) photographs of hybrid xerogel of 20%-NN-M.

Thermogravimetric analysis was used to assess the thermal stability of typical 20%-NN-M and to roughly estimate the amount of loaded amino groups. Fig. 5 shows TG-DTG profiles of both 0-N-M and 20%-NN-M measured under nitrogen environment. An initial weight change of 7.3% and 5.7% are observed for 0-N-M and 20%-NN-M, respectively, which can be assigned to the release of adsorbed moisture. Then both samples decomposed in distinct three steps totalizing weight loss of 16.6% and 18.7%, respectively; and the increased loss for the later one can be related to the incomplete decomposition of (2-aminoethylamino)-propyl once the measurement was carried out using inert atmosphere and similar results was reported by other researches [26]. It can be pointed out that, combined with FT-IR, MAS NMR, TG-DTG and elemental analysis results, amino functional

groups have been introduced into these xerogels employing this single-step sol-gel method, by which enlarged synthesis can be easily manipulated to meet for industrial applications.
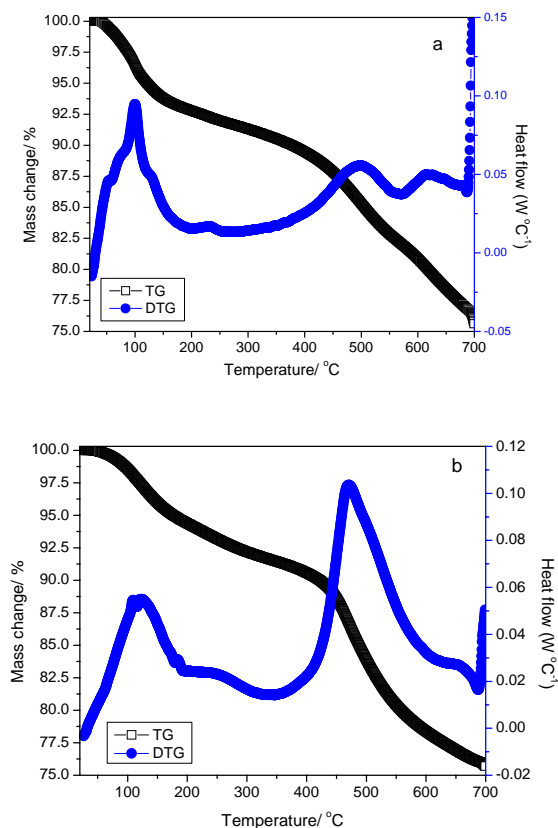

Fig.5. Thermogravimetric (TG) curves of 0-N-M (a) and 20%-NN-M (b)

3.2 Adsorption of Pb^{2+}

It was demonstrated by various techniques as-mentioned that amino groups have been incorporated into the final products. In an attempt to investigate the accessibility of the amino groups in the synthesized materials, adsorption of Pb^{2+} from aqueous solutions by amino-functionalized xerogels was studied at room temperature. As a control, unfunctionalized xerogel (0-N-M) and hexagonally ordered SBA-15 was tested for Pb^{2+} cations binding sites under similar conditions, and the adsorption abilities on purely inorganic SBA-15 and 0-N-M were negligible, which can be exclusively attributed to the absence of active amino groups in both materials (results not shown).

All materials functionalized with monoamine, diamine and triamine organic chains exhibit remarkable metal withdrawal capacities as shown in Table 2, where adsorbed amount and removal percentage of the tested results are displayed. The adsorption results suggest that there are similar sorption performances irrespective of the type of amino ligands; that is, aqueous Pb^{2+} adsorption percentage clearly increases with the amino group content in the adsorbents, revealing amino groups worked as

complexing sites for Pb^{2+} ions under performed conditions. Nevertheless, it should be realized that an inattentive glance to Table 2 may lead to mis-understanding conclusions, i.e. all adsorbents with maximum amino group content exhibited similar adsorption behavior. Considering the fact that, however, the series of NN-M adsorbents with low loading (5~10%)of amino groups displayed relatively higher adsorption capability than another two series; therefore, it implies that the Pb^{2+} cation could form tetrahedral and/or octahedral complexes using flexible numbers of amino groups as ligands. Consequently, the nitrogen anchoring points to metal species number ratio increases with amino group content in these adsorbents.

Table 2. Adsorption capabilities of Pb^{2+} by amino-functionalized xerogels.

Adsorbents	Adsorbed amount (mg.g^{-1})	Removal percentage (%)
5%-N-M	80.3	40.1
10%-N-M	101.9	51.0
20%-N-M	140.4	70.2
30%-N-M	176.4	88.2
5%-NN-M	131.5	65.8
10%-NN-M	150.5	75.3
20%-NN-M	142.4	71.2
30%-NN-M	176.5	88.3
5%-NNN-M	97.1	48.6
10%-NNN-M	147.6	73.8
20%-NNN-M	193.3	96.6
30%-NNN-M	186.1	93.0

4. Conclusion

A single-step sol-gel method was used to synthesize amino-functionalized xerogels using mono-, di-, tri-amino-organoalkoxysilanes, PMHS and TEOS as co-precursors in the absence of traditional organic surfactants. Functional amino groups were incorporated into these porous hybrid xerogels while preserve a desirable pore structure with high surface area and opened pore channels. The amino-functionalized groups in such a porous structure are readily accessible and show favorable affinity toward Pb^{2+} ions with adsorption capacity up to 176.5 mg/g from aqueous conditions, whereas undetectable Pb^{2+} adsorption was observed for non-functionalized xerogel and pure SBA-15. Furthermore, the amount of Pb^{2+} adsorption was increased with the

amount of amino groups incorporated into objective adsorbents, and thus implying that amino groups introduced were accessible within studied synthesis conditions.

References

[1] T. Maschmeyer, Curr. Opin. Solid State Mater. Sci. **3**, 71 (1998).

[2] F. Hoffman, M. Cornelius, J. Morell, M. Froba, Angew. Chem. Int. Ed. **45**, 3216 (2006).

[3] H. Budiman, F. Sri, A. Setiawan, E-J Chem. **6**, 141 (2009).

[4] Z.X. Wu, D.Y. Zhao, Chem. Commun. **47**, 3332 (2011).

[5] K. Inumaru, M. Murashima, T. Kasahara, S. Yamanaka, Appl. Catal. **52**, 275 (2004).

[6] A. Calvo, M. Joselevich, G. Soler-Illia, F.J. Williams, Micropor. Mesopor. Mater. **121**, 67 (2009).

[7] H. Zheng, C. Gao, S. Che, Micropor. Mesopor. Mater. **116**, 299 (2008).

[8] K.Z. Hossain, L. Mercier, Adv. Mater. **14**, 1053 (2002).

[9] S. Saeung, V. Boonamnuayvitaya, Env. Eng. Sci. **25**, 1477 (2008).

[10] S. Kim, J. Ida, V.V. Guliants, J.Y.S. Lin, J. Phys. Chem. B **109**, 6287 (2005).

[11] T. Yokoi, T. Tatsumi, H. Yoshitake, Bull. Chem. Soc. Jpn. **76**, 2225 (2003).

[12] R. Saad, K. Belkacemi, S. Hamoudi, J. Colloid Interf. Sci. **311**, 375 (2007).

[13] B.M. Choudary, M.L. Kantam, P. Sreekanth, T. Bandopadhyay, F. Figueras A. Tuel, J. Mol. Catal. A **142**, 361 (1999).

[14] V. Antochshuk, M. Jaroniec, Chem. Commun. 258 (2002).

[15] H. Schmidt, J. Sol-Gel Sci. Technol. **1**, 217 (1994).

[16] K.S.W. Sing, D.H. Everett, R.A.H. Haul, L. Moscou, R.A. Pierotti, J. Rouquerol, T. Siemieniewska, Pure & Appl. Chem. **57**, 603 (1985).

[17] S. Zhai, L. Zhang, Q. An, B. Zhai, J. Optoelctron. Adv. Mater. **13**, 733 (2011).

[18] J. Aguado, J.M. Arsuaga, A. Arencibia, M. Lindo, V. Gascón. J. Hazard. Mater. **163**, 213 (2009).

[19] T. Yokoi, H. Yoshitake, T. Tatsumi, J. Mater. Chem. **14**, 951 (2004).

[20] N. Igarashi, K. Hashimoto, T. Tatsumi, J. Mater. Chem. **12**, 3631 (2002).

[21] L. Bois, A. Bonhommé, A. Ribes, B. Pais, G. Raffin, F. Tessier, Colloids Surf. A. Physicochem. Eng. Aspects **221**, 221 (2003).

[22] S. Saeung, V. Boonamnuayvitaya, J. Environ. Sci. Health **20**, 379 (2008).

[23] S. Hamoudi, A. El-Nemr, K. Belkacemi, J. Colloid Interface Sci. **343**, 615 (2010).

[24] X. Z. Wang, W. H. Li, G. S. Zhu, S. L. Qiu, D. Y. Zhao, B. Zhong, Microporous Mesoporous Mater. **72**, 87 (2004).

[25] W. Zhu, Y. Han, L. An, Microporous Mesoporous Mater. **71**, 137 (2004).

[26] M.R. Mello, D. Phanon, G.Q. Silveira, P.L. Llewellyn, C.M. Ronconi, Microporous Mesoporous Mater. **143**, 174 (2011).

*Corresponding author: anqingda@dlpu.edu.cn
                        zhaisr@dlpu.edu.cn